Springer

KSME

Journal of Mechanical Science and Technology 32 (9) (2018) 4373~4381
www.springerlink.com/content/1738-494x(Print)/1976-3824(Online)
DOI 10.1007/s12206-018-0836-y

Explicit controller of a single truck stability and rollover mitigation †

Fitri Yakub[1,*], Pauziah Muhammad[1], Hoong Thiam Toh[1], M. Sofian Abu Talip[2] and Yasuchika Mori[3]

[1]*Malaysia-Japan International Institute of Technology, Universiti Teknologi Malaysia, 54100, Kuala Lumpur, Malaysia*
[2]*Department of Electrical Engineering, Faculty of Engineering, University of Malaya, Jalan Universiti, 50603, Kuala Lumpur, Malaysia*
[3]*Transportation Systems & Electric Co., Ltd, 3-13-2, Takadanobaba, Shinjuku, 169-0075, Tokyo, Japan*

(Manuscript Received June 22, 2017; Revised February 15, 2018; Accepted May 10, 2018)

Abstract

This study's aim was to enhance the maneuverability safety in the coordination of active rear steering and differential braking control for untripped rollover prevention, which performs a panic lane change maneuver to bypass the obstacle encountered in the path. In avoiding rollover accidents, there are several guidance preventions, such as to secure the vehicle from the intention of the driver and to position the vehicle in the actual lane. A crosswind effect is also found to be a crucial factor since this may cause other accidents. Therefore, there is a need to monitor the driver's actual path and maintaining the stability of the vehicle along the desired path in order to avoid rollover accidents. We extended the analysis of Yakub and Mori (2015) [1], by suggesting an explicit model of predictive control, which includes an active rear steering and braking control for each wheel. Our main focus was on the general trade-off between rollover prevention and path tracking. The effectiveness of the explicit control model invented for this study was measured and validated by the simulation results for a heavy vehicle proposed in this research.

Keywords: Heavy vehicle; Stability; Rollover; Explicit model predictive control; Rear steering; Braking control

1. Introduction

Many optimal control design approaches depend on dynamic models of the processes to be controlled. Generally, model predictive control (MPC) represents a model based control structure that is commonly used to control constrained linear or nonlinear models, with the inclusion of multivariable models in which a mathematical dynamics process model is employed for the prediction of the future behavior of the model, and the optimization of the control process performance across a prediction horizon [2]. Attributable to its benefits, MPC has been applied in many applications related to automotive systems for many driver assistance and active safety systems, vehicle dynamics-based systems, and collision avoidance and autonomous driving systems, to enhance vehicle stability, ride comfort, as well as to reduce traffic accidents [3-5].

Vehicle rollover accidents are considered among the most fatal vehicle accidents. Rollover crashes account for only about 2 % of all crashes where they constitute roughly one-third of all occupant fatalities. There are about 7500 highway deaths from rollovers each year in the United States and the annual cost associated with rollover injuries and fatalities is about USD50 billion a year [6]. According to the Japan Traffic Accidents Databases, rollover accidents are about one-fifth of the total single-vehicle accidents [7]. Due to the high center of gravity, disturbance effects like gusts of wind, irregularity in road surfaces, and sudden maneuvers, heavy vehicles and trucks have a tendency be involved in rollover accidents. Therefore, it is crucial to implement speed and safety control systems in order to identify and avoid rollover, which would improve vehicle stability.

The detection and prevention of rollover, including active suspension, active braking systems (ABSs), and active stabilizers, have been exhaustively investigated in Refs. [8-10]. The installation of dedicated actuators for the control of active parts is required in this case, although this will increase the vehicle cost. Moreover, numerous control methods, including active front steering (AFS hereafter) [11], active rear steering (ARS hereafter) [12], and four-wheel steering [13], are predicted to form new steering systems that possess stability and maneuverability in situations of high speed during lane changes. These features are needed to avoid emergency situations on a slippery road or curb, reducing the roll rate and the lateral acceleration when turning round a curve.

AFS has a significant impact on the behavior of lateral vehicles in normal driving scenarios. However, this steering no longer has the ability to provide sufficient lateral force with high acceleration, mainly due to the highly nonlinear proper-

*Corresponding author. Tel.: +60 11 5221 4962, Fax.: +60 3 2203 1265
E-mail address: mfitri.kl@utm.my
† Recommended by Associate Editor Ji Seong Jang

ties of the tire. On the other hand, ARS has been proven to be effective in rollover prevention and roll damping on low friction surfaces. In the case of driving in a natural environment (e.g., inclement weather), topographic features and infrastructure must be taken into account. ARS can potentially reduce roll motion; however, it causes the vehicle to move away from the intended trajectory of the driver. Therefore, it is crucial to reduce this deviation from the intended trajectory, and the dynamic behavior of the vehicle simultaneously, which is, as a premise, subject to rollover.

The drawbacks mentioned above can be ameliorated by inventing the MPC controller using an explicit technique which is able to (1) follow as much as possible the desired trajectory, (2) prevent rollover, (3) reject the effect of disturbance, and (4) improve the stability and maneuverability of heavy trucks. The proposed new control technique that uses a linear MPC in a nonlinear vehicle dynamics model to represent the actual vehicle system is the primary contribution of this study. Since the roll dynamics motion is impacted during high speed scenarios, we investigated the truck vehicle with middle forward speed (15 m/s) in a lateral maneuver for a single lane change situation.

At the same time, the ABS concept also emphasizes differential braking control (DBC) to generate the needed corrective longitudinal force and yaw moment via braking forces distribution between the right and left sides of the rear wheels. Only the rear left/right braking is chosen instead of the front/rear braking in order to prevent conflicts or interventions between AFS and DBC commands (which is the second contribution of this study).

The outline of this paper starts with the model concept of a full vehicle, nonlinear tires and disturbances which are explained in Sec. 2. Sec. 3 discusses the control approach for the linear MPC, the rear braking control and an obstacle avoidance maneuvers. Next, Sec. 4 presents the validation of the simulation results, and finally Sec. 5 concludes the finding.

2. Modeling and indicator

2.1 Double-track model

Referring to the same model in Ref. [1] shown in Fig. 1, it consists of the sprung vehicle mass, the suspension, as well as the wheel weights for an unsprung mass; however, the pitch motion is not considered here. A comprehensive discussion of the derivation process is available in Ref. [1].

The following terms are used in the study: F_x and F_y represent the longitudinal and lateral tire forces; F_w and M_w correspond to the force and moment applied by the side wind; F_z represents the normal tire load; M_z describes the total corrective reaction moment from the differential braking factors; x, y and z represent the coordinates of the body frame of the vehicle's position; ω_w is the angular velocity of the tires; v_x and v_y are the longitudinal and lateral wheel velocities; T_b is the wheel torque; δ_f and δ_r are used for the steering angle in the rear and front wheels, respectively; μ is the road adhesion

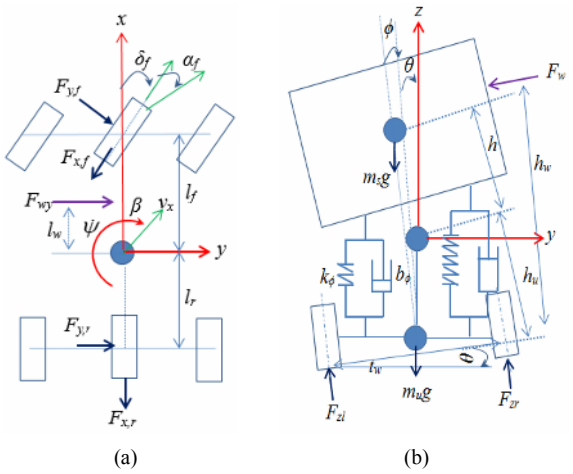

Fig. 1. Single truck model with roll DoF: (a) Top view; (b) front view.

coefficient; ψ represents the yaw/heading angle; $\dot{\psi}$ denotes the yaw rate; β refers to the vehicle's side slip angle; θ denotes the bank angle; ϕ and $\dot{\phi}$ represent the roll and the roll rate angle. Other vehicle parameters are discussed in Ref. [14]. The variables at the front and rear wheels are shown in lower subscripts $(\cdot)_f$ and $(\cdot)_r$.

The motion of the longitudinal, yaw, roll, lateral, and rotational dynamics of the rear and front wheels of 8-DoF for the nonlinear model and vehicle motion are discussed in planar dynamics formulas via the following differential equations:

$$\sum F_x : m(\ddot{x} - \dot{y}\dot{\psi}) = 2F_{xf} + 2F_{xr} - m_s h\phi\ddot{\psi} - 2m_s h\dot{\phi}\dot{\psi} + (l_f - l_r)m_u\dot{\psi}^2 \quad (1)$$

$$\sum F_y : m(\ddot{y} + \dot{x}\dot{\psi}) = 2F_{yf} + 2F_{yr} + m_s h\ddot{\phi} - m_s h\phi\dot{\psi}^2 - m_s h\phi\dot{\phi}^2 + (l_r - l_f)m_u\ddot{\psi} + F_w \quad (2)$$

$$\sum M_z : I_{zz}\ddot{\psi} - I_{xz}\ddot{\phi} = t_w/2\,(-F_{xf,l} + F_{xf,r} - F_{xr,l} + F_{xr,r}) + 2l_f F_{yf} - 2l_r F_{yr} + (l_r - l_f)m_u(\ddot{y} + \dot{x}\dot{\psi}) + M_w \quad (3)$$

$$\sum M_x : (I_{xx} + m_s h^2)\ddot{\phi} + m_s h(\ddot{y} + \dot{x}\dot{\psi}) - I_{xz}\ddot{\psi} = m_s gh\phi - 2k_\phi\phi - 2b_\phi\dot{\phi} \quad (4)$$

$$J_b\dot{\omega}_{wi} = -r_w F_{xi} - T_{bi} - b_w\omega_i, \quad i = (f, r). \quad (5)$$

The inertial trajectory of the vehicle (X, Y) at the time t, from the current position (X_0, Y_0) is presented as follows:

$$X = X_0 + v_x\int_0^t \cos(\beta + \psi)\,dt, \quad (6)$$

$$Y = Y_0 + v_x\int_0^t \sin(\beta + \psi)\,dt, \quad (7)$$

where we select the start position (X_0, Y_0) as zero hereafter.

The objectives of this study involve rollover prevention, vehicle yaw stability control, and lane change maneuver. Thus, the target yaw rate and vehicle slip angle have to fulfil the upper bound limit:

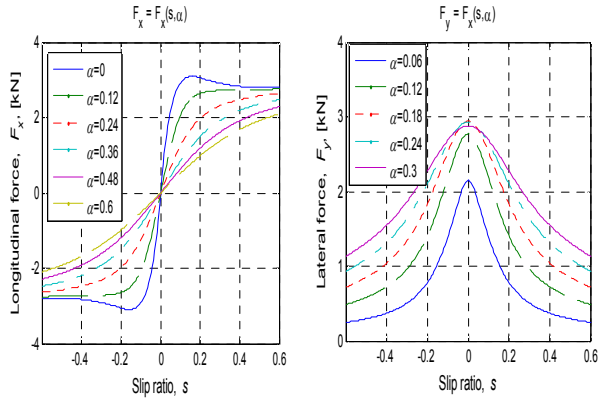

(a) (b)

Fig. 2. Semi-empirical tire model: (a) Longitudinal; (b) lateral forces.

$$\dot{\psi}_{des} \le \mu g / v_x , \quad \beta_{des} \le \tan^{-1}(0.02\,\mu g) , \tag{8}$$

where the intended yaw rate response is not always obtained in the case of tire force exceeds its adhesion limit. Therefore, it has an upper bound limit [15].

2.2 Nonlinear tire model

The tire dynamics is taken into account for the vehicle model because the only contact between the road surface and the vehicle is through the tires. The most widely applied existing nonlinear tire model applications and structures are from the main parameters and analytical considerations one the basis of the on tire data measurements which are referred to the 'semi-empirical tire model', or 'Pacejka tire model' [16]. Therefore, for this study a combination semi-empirical tire model was used.

Figs. 2(a) and (b) illustrate the tire forces at different longitudinal tire slip ratios and lateral slip angles, respectively. The nonlinear tire should satisfy the following equation:

$$\sqrt{F_{xi}^2 + F_{yi}^2} \le \mu F_{zi} , \qquad i = (f, r). \tag{9}$$

The nonlinear kinematics related to the tire slip angles for the front and rear wheels, and the longitudinal tire slip ratio, are given as follows,

$$\alpha_f = \delta_f - \tan^{-1}\left(\frac{\dot{y} + l_f \dot{\psi}}{\dot{x}}\right), \quad \alpha_r = \delta_r - \tan^{-1}\left(\frac{\dot{y} - l_r \dot{\psi}}{\dot{x}}\right), \tag{10}$$

$$s = 1 - \frac{v_x}{r_w \omega_w} , \quad \text{Acceleration if } r_w \omega_w \ge v_x , \tag{11}$$

$$s = \frac{r_w \omega_w}{v_x} - 1 , \quad \text{Braking if } r_w \omega_w \le v_x . \tag{12}$$

2.3 Aerodynamic force and moment

The disturbance effect on the vehicle's stability is crucial, since bumpy or irregular roads can give additional force and torque, which aid in the resistance of the overturning forces. Here, we consider the front steering angle to be a disturbance for the system because the effect of driving in a sudden maneuver, prior to work by Ref. [1], and this assumption involving the front steering angle.

The effect of wind on the vehicle's stability is critical, as a strong wind from the outward or inward side can provide the additional force or torque needed to help to resist the overturning forces. However, this study only considers the effect of wind on lateral and yaw motions, as in Ref. [17]. The effect of wind on longitudinal motion is not considered.

2.4 Load transfer ratio

Load transfer ratio (LTR) is assumed to be the most dependable rollover indicator, irrespective of operational conditions and vehicle configurations. It is employed to identify the onset of the rollover in this study. More details on LTR are discussed in Ref. [18]. The LTR is defined as the overall load difference between the left and right wheels of the vehicle, which are normalized by the total load:

$$LTR = \frac{F_{zr} - F_{zl}}{F_{zr} + F_{zl}} , \tag{13}$$

where F_{zl} and F_{zr} refer to the vertical tire forces that act on the left right and left side wheels. Two-wheel lift off of one particular side of the vehicle takes place in the case LTR is 1 or -1. We assume LTR is the rollover threshold and is in the range of -1 and 1. We created a torque balance around the horizontal roll axles with respect to the suspension torques, and the vertical wheel forces by assuming unsprung mass and lateral load transfer due to the effect of lateral acceleration:

$$LTR = \frac{2\left[c\dot{\phi} + k\phi + h_{uf} m_u (\ddot{y} + v_x \dot{\psi} - h\ddot{\phi})\right]}{mg\, t_w} , \tag{14}$$

where m_u represents the vehicle's unsprung mass, t_w represents the width of the vehicle, and h_u represents the roll center distance under the sprung mass. The nonlinear motions of the vehicle in Eqs. (1)-(12) are described by the compact differential equation:

$$\dot{\xi} = f\,(\xi, u,\ \omega_d, r_{des}), \qquad \eta = h\,(\xi) , \tag{15}$$

where the state for the input, disturbance, reference and output vectors are as follows:

$$\begin{aligned}
&\xi = [v_y\ Y\ X\ \dot{\psi}\ \psi\ \dot{\phi}\ \phi\ \omega_{f,l}\ \omega_{f,r}\ \omega_{r,l}\ \omega_{r,r}]^T , \\
&u = [\delta_r], \qquad ARS \\
&u = [\delta_r\ \rho_{r,l}\ \rho_{r,r}]^T , \quad ARS\ +\ DBC \\
&\omega_d = [\delta_f\ F_w\ M_w]^T , \ r_{des} = [Y_{des}\ \ LTR_{des}]^T , \ h(\xi) = [Y\ \ \psi\ \ \phi\ \ \dot{\phi}]^T .
\end{aligned} \tag{16}$$

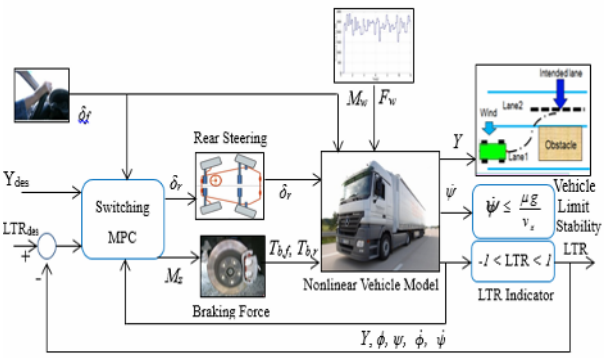

Fig. 3. Explicit MPC through ARS with DYC system.

The values of the state variables in Eq. (16) such as yaw rate can be measured by yaw rate sensors in the form of microelectromechanical sensor units. Some hard/expensive to measure vehicle variables can be estimated using other on-vehicle sensors. The roll rate can be estimated directly using a GPS attitude system, in combination with an automotive grade gyroscope oriented to measure the roll rate. As a consequence, the roll angle is calculated from the measured roll rate.

The reason to include the disturbance vector is because the aim to investigate whether any other controller methods can be designed to prevent worse scenarios that may occur in real world situations. The estimation process is not considered here as the state variable can be measured or estimated through using commercially available tools.

In this paper, we assume all disturbances are known *a priori* and are given at the specific time during travelling as illustrated in Fig. 5. In addition, we designed the controller with the best control technique based on the fatal crash scenario so that it will at least prevent the passengers and driver from being injured.

3. Controller scheme

3.1 Implicit model predictive control

A block diagram of the MPC controller design is shown in Fig. 3. The task of MPC is to monitor the lane in the single lane change maneuver by the help of ARS and ABS to prevent rollover.

In this paper, the nonlinear vehicle given in Eqs. (1)-(5) is linearized based on the assumption that the vehicle's forward speed is constant. The linearized model is a satisfactory approximation to the behavior of the actual nonlinear vehicle model under certain operating conditions. MPC is designed on the basis of 3-DoF lateral-roll motions:

$$m\dot{v}_y = \frac{1}{I_{xx}v_x}[-(C_r + C_f)J_{xq}\,v_y + ((C_r l_r - C_f l_f)J_{xq} - I_{xx}mv_x^2)\dot{\psi}] - \frac{1}{I_{xx}}[m(hb_\phi)\dot{\phi} - mh(mgh - k_\phi)\phi - C_f J_{xq}\,\delta_f + C_r J_{xq}\,\delta_r] \tag{17}$$

$$I_{zz}\ddot{\psi} = \frac{1}{v_x}[(C_r l_r - C_f l_f)\,v_y - (C_f l_f^{\,2} + C_r l_r^{\,2})\dot{\psi}] + C_f l_f\,\delta_f - C_r l_r\,\delta_r - \frac{t_w p_i}{2} \tag{18}$$

$$I_{xx}\ddot{\phi} = \frac{h}{v_x}[(C_r l_r - C_f l_f)\,\dot{\psi} - (C_f + C_r)v_y] - b_\phi\dot{\phi} + (mgh - k_\phi)\phi + C_f h\,\delta_f + C_r h\,\delta_r. \tag{19}$$

The motions of the vehicle in Eqs. (17)-(19) are represented by a state-space arrangement with $\dot{x} = [\dot{v}_y\ \dot{Y}\ \ddot{\psi}\ \dot{\psi}\ \dot{\phi}\ \phi]^T$ as follows:

$$\dot{x} = Ax + B_1 u + B_2\,\omega_d + B_3\,r_{des}, \quad y = Cx + Du\ . \tag{20}$$

Since the MPC is designed on the basis of a mathematical model of the plant using discrete time, the vehicle dynamics are discretized in Eq. (21) with the application of a Euler approximation method, and neglecting any unmeasured disturbance, to get:

$$\begin{aligned} x_l(k+1|k) &= A_l\,x_l(k|k) + B_l\,u_l(k|k) + B_2\,\omega_{dl}(k|k), \\ y_l(k|k) &= C_l\,x_l(k|k) + D_l\,u_l(k|k) \end{aligned} \tag{21}$$

where $x_l(k|k)$ represents the state vector at a time step k, $x_l(k+i|k)$ represents the state vector at a time step k+1, and $x_l(k|k) \in \mathrm{R}^{x(k|k)}$, $u_l(k|k) \in \mathrm{R}^{u(k|k)}$, $\omega_{dl}(k|k) \in \mathrm{R}^{\omega d(k|k)}$ and $y_l(k|k) \in \mathrm{R}^{y(k|k)}$ represent the state, the control input, the measured disturbance, and the measured output vectors, respectively. Next, we define the following equation:

$$\begin{aligned} &x_l(k) = [v_y\ Y\ \dot{\psi}\ \psi\ \dot{\phi}\ \phi]^T, \quad u_l(k) = [\delta_r\ \rho_{r,l}\ \rho_{r,r}]^T, \\ &\omega_{dl}(k) = [\delta_f], \qquad y_l(k) = [Y\ \ LTR]^T. \end{aligned} \tag{22}$$

The aim of the predictive control system is to determine the optimal control input vector $\Delta\tilde{u}_l\,(k+i|k)$ so that the error function between the reference signal and the predicted output is reduced. The predictive control system's optimization is addressed by reducing the cost function, which is given by:

$$Min: J_{mpc}(k) = \sum_{i=1}^{H_p}\left\|\overline{y}_l(k+i) - r_{des}(k+i)\right\|^2_{S_q(i)} + \sum_{i=0}^{H_c-1}\left\|\Delta\overline{u}_l(k+i)\right\|^2_{S_r(i)} \tag{23}$$

where the first summation of the given cost function reflects the reduction of trajectory tracking errors in the difference between the predicted outputs $\tilde{y}_l\,(k+i|k)$, $(i = 0,\ldots, H_p\text{-}1)$ and the output reference signals $r_{des}\,(k+i|k)$, $(i = 0,\ldots, H_p\text{-}1)$. The second summation in Eq. (23) is used to give a penalty to the control signal effort in the rear steering angle $\Delta\tilde{u}_l\,(k+i|k)$, $(i = 0,\ldots, H_c\text{-}1)$ of the active rear steering control maneuver. In this

case, r_{des} $(k+i|k)$ comprises the reference value of the yaw angle and lateral position.

The difference in the rear steering angle $\Delta\tilde{u}_l$ $(k+i|k)$ is given in the case where the cost function is at its minimum value. The weight matrices $S_q(i)$ and $S_r(i)$ are semi-positive definite, and positive definite, respectively, and can be tuned for any desired closed-loop performance. $S_q(i)$ is defined as the state tracking weight, since the error $\tilde{y}_l$ $(k+i|k)$ - r_{des} $(k+i|k)$ can be made as small as possible by increasing $S_q(i)$.

In a similar fashion, $S_r(i)$ represents the input tracking weight and the variation of the input is decreased to slow down the response of the system by increasing $S_r(i)$. The predictive and control horizon are typically considered to be $H_p \geq H_c$, while the control signal is considered constant for $H_c \leq i \leq H_p$. The optimization of the predictive control system is formulated via the cost function in Eq. (23), which takes into account the constraints of an actuator, and is defined as follows:

$$
\begin{aligned}
&\min_{\Delta U_k} \quad J(x_l(k), \Delta U_{lk}) \\
&subject\ \ to: \\
&\quad \hat{x}_l(k+1|k) = A_l x_l(k|k) + B_l u_l(k|k) + B_2\, \omega_{dl}(k|k) \\
&\quad \hat{x}_l(k+2|k) = A_l \hat{x}_l(k+1|k) + B_l \hat{u}_l(k|k) + B_2\, \hat{\omega}_{dl}(k|k) \\
&\qquad\qquad \vdots \\
&\quad \hat{x}_l(k+i|k) = A_l \hat{x}_l(k+i-1|k) + B_l \hat{u}_l(k+i-1|k) \\
&\qquad\qquad + B_2\, \hat{\omega}_{dl}(k+i-1|k) \\
&\quad \delta_{r,\min} \leq \hat{u}_{1l}(k+i|k) \leq \delta_{r,\max} \\
&\quad \Delta\delta_{r,\min} \leq \Delta\hat{u}_{1l}(k+i|k) \leq \Delta\delta_{r,\max} \\
&\quad \rho_{i,\min} \leq \hat{u}_{2l}(k+i|k) \leq \rho_{i,\max} \\
&\quad \Delta\rho_{i,\min} \leq \Delta\hat{u}_{2l}(k+i|k) \leq \Delta\rho_{i,\max} \\
&\quad Y_{\min} \leq \hat{y}_{1l}(k+i|k) \leq Y_{\max} \\
&\quad LTR_{\min} \leq \hat{y}_{2l}(k+i|k) \leq LTR_{\max}, \quad i = 1, \cdots H_p .
\end{aligned}
\tag{24}
$$

The maximal tire slip angle $\alpha_{r,max}$ is detected when the maximal tire force is achieved in order to prevent extreme saturation of the tire lateral force:

$$
\delta_{r,\max}(k) = \alpha_{r,\max} + \frac{v_y + l_r\dot{\psi}}{v_x} . \tag{25}
$$

The inequality of tire slip angle; $-\alpha_{\lim} < \alpha_r < +\alpha_{\lim}$ indicates that the tire steer angle, δ_r, may be held within a bound of the vehicle side slip angle, β_r, to avoid the lateral tire force saturation region. Thus, these bounds are determined once at time k such that $\alpha_{r,max}$, $(k+i|k)$ is equal to constant. Before the upper and lower bounds are defined, the linearization of the nonlinear tire model is investigated at the operating point $\alpha_{r,0}$, $F_{yr,0}$.

$$
F_{y,r} = (\alpha_r - \alpha_{r,0}) \times k_{\alpha,r} + F_{y,r,0} , \tag{26}
$$

where $k_{\alpha r}$ denotes the linearization coefficient. Next, an optimal input was computed for the following time step rather than being calculated for the immediate time step, by addressing convex optimization problems during each time step. Later, the first input was applied on the plant in Eq. (21), and the others were rejected, which yielded the optimal control sequence as follows:

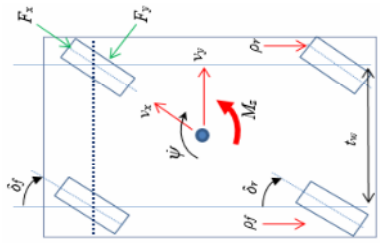

Fig. 4. Differential braking control.

$$
u(t) = u_0^*(x(t)) . \tag{27}
$$

An implicit MPC solves a quadratic program (QP) at each control interval to determine the optimal manipulated variable Δu_{lk} adjustments. These adjustments are the solution of the implicit nonlinear function $u = f(x)$. The optimization problem in Eq. (24) is iterated with the new value at a time k+1 via new state $x(k+1)$, and all orders are then updated.

3.2 Braking control algorithm

The required direct yaw moment control M_z is obtained from the variation between the two sides of the vehicle torque, as in Eq. (5). In this research, the braking torque is only used based on the yaw rate. Thus, it is only activated in the case where the vehicle moves toward instability or in emergency maneuvers, since it impacts the longitudinal motion, while the rear steering angle is assumed for the total maneuver to be in control or in standard driving maneuvers. We took into account two control inputs, rear steering angle, as well as differential braking at rear right and left tire, but only one control input is used at a time [19] as illustrated in Fig. 4.

For the braking control law design, we employed only rear wheels at a time to produce the control moment by applying the difference in braking among the two axles: $\Delta T_{b,r} = T_{b,rl} - T_{b,rr}$. Since the front steering angle command acts as a driver abrupt maneuver disturbance, the braking torque is only applied to the rear wheels and the control law is designed as:

$$
T_{b,rl} = 0, \quad T_{b,rr} = \frac{-2M_z r_w}{t_w}, \quad if\ \Delta T_{b,r} < 0, \quad \dot{\psi} > 0 , \tag{28}
$$

$$
T_{b,rl} = \frac{2M_z r_w}{t_w}, \quad T_{b,rr} = 0, \quad if\ \ \Delta T_{b,r} > 0, \quad \dot{\psi} < 0 . \tag{29}
$$

Eqs. (28) and (29) were chosen because the brake torque applied to the rear wheel must be positive. We used only braking force ρ to realize the rollover prevention by considering

the differential braking force acting either on the left or right side of the wheel as:

$$\rho_i = \frac{t_w}{2J_{zz}} \ . \tag{30}$$

The difficulty and issue now turns into how to tune and determine the controller weighting matrices S_q and S_r in order to avoid poor response by surpass control input saturation, beyond the location and bandwidth limitations of the actuators.

3.3 Explicit predictive control

The control allocation issue is defined as a nonlinear optimization one, in which an explicit piecewise affine (PWA) linear approximate solution operation is calculated off-line [20] for a predefined set of operating conditions rather than on-line for nominal MPC (implicitly, as discussed in Sec. 3.1). This method is highly effective for issues with a small amount of states, simplistic constraints and a modest horizon to obtain a convenient set of regions.

The concept of explicit MPC involves solving the optimization issue in Eq. (24) off-line for all $x(t)$ in a set X by applying a multi-parametric quadratic program (mpQP) [21, 22]. Models in mpQP that are applied to arrive at explicit solutions to the MPC problems accomplish online MPC functionality without the need to solve optimization problems during every time step. We consider the polytopic function to be:

$$X = \left\{ x \in \Re^n : S_1 x \le S_2 \right\} \subset \Re^n \ . \tag{31}$$

Depending on the performance index in Eq. (23), and the set of constraints in Eq. (24), with some modification, the mathematical problems can be defined as follows:

$$\begin{aligned} &\min_{U_k} \quad \frac{1}{2} U_k{}^T H U_k + x_k^T F^T u_k \\ &subject \ \ to: \\ &\quad G u_k \le W + K x_k \end{aligned} \tag{32}$$

where the matrices H, G, F, W and K correspond to the function of the controller weighting matrices S_q, S_r and the limits $\tilde{u}_{l,min}$, $\tilde{u}_{l,max}$, $\tilde{y}_{l,min}$, $\tilde{y}_{l,max}$. The considerations on weighting matrices S_q and S_r are usually satisfied by selecting S_q and S_r as diagonal matrices that conveniently penalize the relative importance of the state or the input values.

The issue in Eq. (32) can be seen as an mpQP in U_k, where x_k is a vector of parameters, as follows:

$$z = U_k + H^{-1} F^T x_k \ , \tag{33}$$

where z is the optimization variable vector, $z = [u_0{}^T \ u_1{}^T \ldots . \ u_{Hc\text{-}1}{}^T]^T$. The issue in Eq. (32) can then be redefined as:

$$\begin{aligned} &\min_{z} \quad \frac{1}{2} z^T H z_k \\ &subject \ \ to: \\ &\quad G z \le W + S x_k \ . \end{aligned} \tag{34}$$

This is an mpQP in z, parameterized by x_k. The matrix S is given as $S = E + GH^{-1}F^T$. To make explicit the dependence of u_k on x_k, rather than implicit by using the optimization procedure that addresses the issue in Eq. (24), the MPC defined by Eqs. (24) and (27) can be written in the form of a discrete piecewise affine function as follows:

$$u(k) = \begin{cases} F_1 x_k + G_1 \ if \ H_1 x_k \le k_1 \\ \quad \vdots \qquad \vdots \\ F_m x_k + G_m \ if \ H_m x_k \le k_m \end{cases} \tag{35}$$

where x_k, $k = 1,\ldots, m$ is polyhedral regions, each defined by its own set of linear inequalities. As a consequence, on-line calculations are decreased to the simple evaluation of Eq. (35), and can be applied in fast sampling applications. The mpQP in z can be addressed offline for the intended state space area. Calculating the control input at a time step k becomes a simpler task. An advantage of the explicit solution is that the online solution can be computed faster than solving the QP numerically if the number of regions, m, is small.

Thus, the explicit MPC is the procedure that allows, in the special case described by Eq. (24), to explicitly express the control law Eq. (27) obtained through the solution to Eq. (24) and the application of the receding horizon principle. Thus, in the presence of the same design parameters (i.e., weight matrices, prediction and control horizons, constraints in input and output), Eqs. (27) and (35) coincide and must give rise to the same simulation results.

4. Simulation

4.1 Scenario description

The controllers of the proposed methods are applied to a vehicle path moving on a single lane change for the thread avoidance case. The vehicle is assumed to be travelling horizontally towards the path with v_x = 15 m/s without accelerating or braking. The common obstacle avoidance maneuver is simulated with a peak driver steering input with a magnitude of 10 degree, so δ_f in the initial driving conditions is considered to move in the direction of the path at t = 2 second, playing the role of a measurable disturbance on the vehicle. The δ_f disturbance is considered to be persistent across the simulation time.

The torque and drag force under the initially defined driving conditions are considered to move in the direction of the path at t = 1 second, with v_w = 10 m/s, as a disturbance on the vehicle. The forces and torques generated through this sidewise-acting gust of wind are considered to be persistent, and are implemented as step functions across the simulation time. Simulations were carried out using the Explicit Model Predic-

tive Control Toolbox that is available in Matlab and Simulink version 2014b, within 15 seconds.

In this case, we compared the overall performance of the controller design for rollover prevention, lateral position, and yaw stability control, without the controller, as well as with the proposed method. We defined the single lane change maneuver at 10 degree step input to represent 10 meters, starting from $t = 0.5$ second or $Y_{ref} = 10$ meter, $LTR_{ref} = 0$, and the yaw stability limit is fulfilled by $\dot{\psi} \leq \mu g / v_x \approx 0.65$ degree/second.

Table 1 shows the numerical values of the truck vehicle's parameters used in this study and their definitions. Table 2 presents the MPC parameters with weighting matrices implemented in ARS for the DYC maneuver cases, with and without explicit methods applied.

Table 1. Heavy vehicle parameters of a single truck [14].

Parameter	Value
m [kg]	14300
m_s, m_u [kg]	1200, 400
I_{xx}, I_{zz}, I_{xz} [kgm^2]	4718, 34917, 166
l_f, l_r [m]	1.95, 1.54
h, t_w [m]	1.15, 1.86
b_ϕ [Nms], k_ϕ [Nm]	100000, 457000
C_f, C_r	582000, 783000
g [m/s^2]	9.8

Table 2. MPC design parameters.

Parameter	MPC
H_p, H_c	11, 5
T_s [s]	0.05
δ_f, $\Delta\delta_f$ [rad, rad/s]	±0.5, ±0.4
M_z, ΔM_z [Nm, Nm/s]	±1500, ± 000
Y, LTR [m, -]	$0 < Y < 10$, ±1
R_1, R_2, ΔR_1, ΔR_2	0.1, 0.1, 0.03, 0.03
Q_{11}, Q_{22} (v_x = 15 m/s)	0.035, 0.155

4.2 Results and discussion

Fig. 5 depicts the responses of the vehicle motions without a controller in the system. Clearly, with no controller, the single lane change maneuver failed to follow the trajectory, causing a collision. The response of LTR motion suggests that the vehicle is unstable, and one side of the tire is not in contact with the ground, while the trajectory is moving, as shown from its steady-state position. The simulation results also show that the yaw stability for the vehicle is worse after five seconds, and gradually becomes more unstable by exceeding stability limit. Furthermore, note that the lateral acceleration of the vehicle is unstable as it becomes infinite after five seconds.

Fig. 6 shows the vehicle's responses with the controller to ARS with a DBC maneuver control, either without or with the explicit method applied. In this particular simulation, we inspect the benefits of the explicit MPC under the predefined disturbances. Both methods clearly perform very well for LTR response, which demonstrates that both sides of the wheels are in contact with the ground, and no rollover occurs during the maneuver under the disturbance. Both methods of control function well in a lateral position response or thread avoidance, indicating the vehicle's lateral position is at a value of 10 meters. For both outputs responses, LTR and Y-position responses, the explicit MPC provides a slightly better response than ARS and DBC in combination.

On the other hand, for the yaw rate response, it was demonstrated that ARS with DBC shows the vehicle's yaw stability is more than ± 0.65 degree/second, and exceeds the limit of the yaw stability. The explicit MPC maintained the vehicle's stability within the predefined stability range. This suggests that DBC is highly influential to control the lane change maneuver at reference via the explicit method when compared to the combination of both input variables. Fig. 6 also shows that the lateral acceleration for both methods control is relatively stable at the steady state of the acceleration of zero. Moreover, based on the control signal responses, all of the maneuvers control under the active constraints in terms of the ARS and

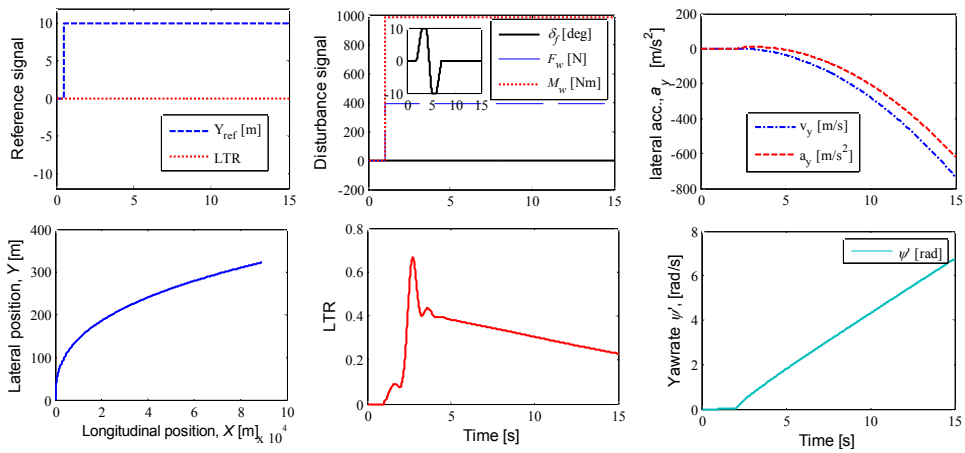

Fig. 5. References and disturbances with the performances of the *v*ehicle without controller.

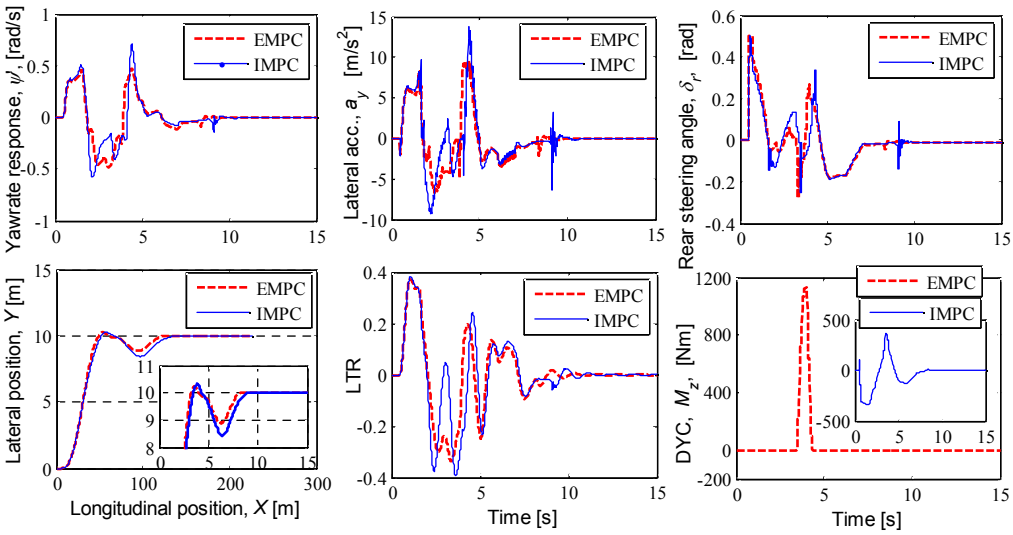

Fig. 6. Vehicle performances with implicit and explicit predictive control of ARS and DBC maneuver control.

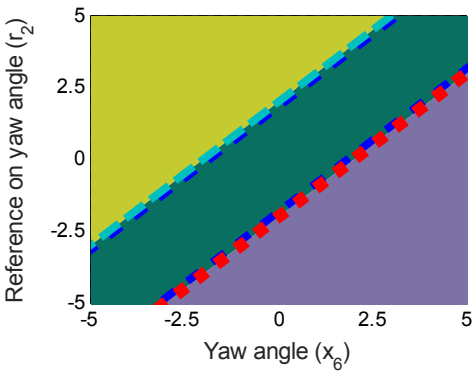

Fig. 7. Piecewise affine partition in 2-D section characterized by the explicit MPC control law.

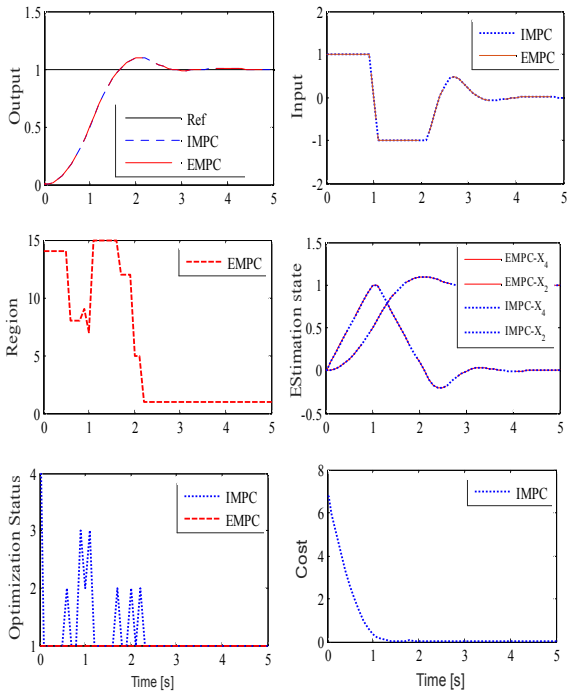

Fig. 8. Region portion, computational cost and optimization and estimates states of implicit and explicit predictive control.

DBC maneuver, which demonstrates the benefits of the MPC method that can be applied in a multivariable system.

Fig. 7 depicts the 2D section of the piecewise affine portion that is determined away from the explicit MPC control law. This polyhedral part is based on yaw angle's feedback, while the remaining parameters remain within range.

The computational time of the explicit solution is determined by the number of possible combinations of active constraints in the QP problem, which is related to the number of regions m. If an explicit solution has many active constraints, significant computational time is needed. In this case, an implicit solution may be preferable. Fig. 8 illustrates the region portion of explicit solution, implicit computational cost, estimates states, and optimization status of both method. The computation effort in Eq. (35) only involved the check of linear inequalities to determine the current region and computing the associated affine function of the current state.

Using the Explicit MPC Toolbox with ten inequalities, the explicit solution of $x(k)$ for m = 3224 is generated in about 234.5 seconds offline computing time.

5. Conclusions

An explicit model predictive control method for heavy vehicle stability and rollover prevention was proposed in this study. This novel control method was evaluated and compared with the conventional MPC (i.e., implicit). An integrated control method for an ARS and ABS maneuver in a heavy vehicle in a thread avoidance case was also examined. These studies consider the front wheel steering and wind gust as disturbances for a vehicle moving forward with a middle speed in a single lane change.

An ARS that uses the rear steering command, and an ABS

that uses the differential rear braking, were designed based on the explicit MPC via the 3-DoF vehicle model with linear tire approximation. The simulation results reveal that the explicit MPC performs better compared to the implicit MPC. The results also demonstrate that the left and right wheel brakes equipped with the ABS are more effective, and have been successfully implemented with a combination of ARS for vehicle steering maneuvers, even in the presence of a disturbance in the yaw and lateral motions.

The improvement of this control method with various combinations like active roll, active suspension, and braking with rear and front tires can be taken into account in further work. The proposed approach will be applied in real-world applications in the near future.

Acknowledgments

This work is supported by Transportation Systems & Electric Co. under grant number KAKENHI 16K06422. First author would like to thank the reviewers for valuable suggestions.

References

[1] F. Yakub and Y. Mori, Heavy vehicle stability and rollover prevention via switching model predictive control, *Int. J. of Innovative Computing, Information and Control,* 11 (5) (2015) 1751-1764.

[2] S. J. Qin and T. A. Badgwell, An overview of industrial model predictive control technology, *Chemical Process Control*, 93 (1997) 232-256.

[3] S. A. Birrell, M. Fowkes and P. A. Jennings, Effect of using an in-vehicle smart driving aid on real-world driver performance, *IEEE Trans. on Intelligent Transportation Systems*, 15 (4) (2014) 1801-1810.

[4] N. Strand, J. Nilsson, I. C. MariAnne Karlsson and L. Nilsson, Semi-automated versus highly automated driving in critical situations caused by automation failures, *Transportation Research Part F,* 27 *Part B* (2014) 218-228.

[5] W. J. Manning and D. A. Crolla, A review of yaw rate and sideslip controllers for passenger vehicles, *Trans. of the Institute of Measurement and Control*, 29 (2007) 117-135.

[6] *http://news.virginia.edu/content/* (2016).

[7] *http://www.itarda.or.jp/english/e_outline1.php* (2014).

[8] H. Mirzaeinejad and M. Mirzaei, Optimization of nonlinear control strategy for anti-lock braking system with improvement of vehicle directional stability on split-μ roads, *Trans. Research Part C*, 46 (2014) 1-15.

[9] R. Tchamna, E. Youn and I. Youn, Combined control effects of brake and active suspension control on the global safety of a full-car nonlinear model, *Vehicle System Dynamics*, 52 (1) (2014) 69-91.

[10] J. Takahashi, M. Yamakado and S. Saito, Evaluation of preview G-vectoring control to decelerate a vehicle prior to entry into a curve, *Int. J. of Automotive Technology*, 14 (6) (2013) 921-926.

[11] J. Yoon, W. Cho, J. Kang, B. Koo and K. Yi, Design and evaluation of a unified chassis control system for rollover prevention and vehicle stability improvement on a virtual test track, *Control Eng. Practice*, 18 (6) (2010) 585-597.

[12] Y. Liu and J. Jiang, Optimum path-tracking control for inverse problem of vehicle handling dynamics, *J. of Mechanical Science and Technology*, 30 (8) (2016) 3433-3440.

[13] A. Tavasoli, M. Naraghi and H. Shakeri, Optimized coordination of brakes and active steering for a 4WS passenger car, *ISA Trans*, 51 (5) (2012) 573-583.

[14] F. Yakub, S. Lee and Y. Mori, Comparative study of LQR and MPC control method with disturbance observer for rollover prevention in inclement environments, *J. of Mechanical Science and Technology*, 30 (8) (2016) 3835-3845.

[15] E. J. Bedner and W. G. Chester, Methods, systems, and computer program products for tire slip angle limiting in a steering control system, *U.S. Patent No. 7,756,620* (2010).

[16] H. B. Pacejka, *Tire and vehicle dynamics*, 3rd Ed., Elsevier, Oxford (2012).

[17] T. Keviczky, P. Falcone, F. Borrelli, J. Asgari and D. Hrovat, Predictive control approach to autonomous vehicle steering, *Proc. Amer. Cont. Conf*., MN, U.S. (2006) 4670-4675.

[18] A. F. Jahromi, W. F. Xie and R. B. Bhat, Robust control of nonlinear integrated ride and handling model using magnetorheological damper and differential braking system, *J. of Mechanical Science and Technology*, 30 (7) (2016) 2917-2931.

[19] F. Yakub and Y. Mori, Enhancing path following control performance of autonomous ground vehicle through coordinated approach under disturbance effect, *IEEJ Trans. on Electronics, Information and Systems*, 135 (1) (2015) 102-110.

[20] T. A. Johansen, I. Petersen and O. Slupphaug, Explicit suboptimal linear quadratic regulation with state and input constraints, *Automatica*, 38 (7) (2002) 1099-1111.

[21] A. Alessio and A. Bemporad, A survey on explicit model predictive control, L. Magni, D. M. Raimondo and F. Allgower (Eds), Nonlinear model predictive control: Towards new challenging applications, *Lecture Notes in Control and Information Sciences*, 384 (2009) 345-369, Springer-Verlag, Berlin, Heidelberg, Germany.

[22] A. Bemporad, M. Morari, V. Dua and E. N. Pistikopoulos, The explicit linear quadratic regulator for constrained systems, *Automatica*, 38 (1) (2002) 3-20.

Fitri Yakub received his Dip.Eng. and B.Eng. degrees in Mechatronics Engineering and Electronics Engineering from University of Technology Malaysia in 2001 and 2006, respectively. He obtained M.Sc. and Ph.D. degrees in Mechatronics Engineering from International Islamic University Malaysia and Tokyo Metropolitan University in 2011 and 2015. He is now with Malaysia-Japan International Institute of Technology. He is a senior member of IEEE and member of IET and SAE. He was recipient of an Asian Human Resource Fund by Tokyo Metropolitan Government from 2012 to 2015. E-mail: mfitri.kl@utm.my.